# Macroscopic Models for a Mushy Region in Concrete Corrosion

Christos V. Nikolopoulos
*Department of Mathematics, University of the Aegean, Karlovasi, 83200, Samos, Greece.*

February 17, 2014

**Abstract.**
Macroscopic models for the corrosion of concrete due to sulphation, describing the formation of a mushy region, are derived and studied by expanding further previous related studies. These models are derived from averaging with the use of the multiple scales method applied on microscopic Stefan - type problems, to capture the effects of the microscopic transformation of calcite into gypsum. The resulting macroscopic model for the diffusion and production of the sulphate inside the concrete is coupled with a time dependent Eikonal equation describing the evolution of the reaction at each point of the concrete wall. In certain cases and for specific geometries of the microstructure, the Eikonal equation admits analytical solutions and the model takes the form of a macroscopic non-local problem. The models derived are solved numerically with the use of a finite element method and the results for various microstructure geometries in the microscale are presented.

**Keywords:** Sulphide Corrosion, Concrete Corrosion, Moving Boundary Problems, Perturbation Methods, Eikonal Equation.

## 1. Introduction

Corrosion of calcite from hydrogen sulfate and its transformation to gypsum is a very interesting phenomenon and its study is essential for the understanding of a lot of processes such as sewer pipes corrosion, monument's corrosion, building decay (failures in building fabric caused by corrosion) etc. ([1], [2]).

The basic reaction describing the fact that $H_2SO_4$ reacts with calcite $CaCO_3$ forming gypsum $CaSO_4 \cdot 2H_2O$ and causing the corrosion of the concrete, is the following:

$$2H_2O + H^+ + SO_4^{2-} + CaCO_3 \xrightarrow{K_c} CaSO_4 \cdot 2H_2O + HCO_3^-.$$

A model for this reaction in the form of a macroscopic moving boundary problem, was presented initially in [1] and it was further studied in a series of papers as in [3], [4] etc. In addition an extensive study of the problem of corrosion by sulphate has been also presented in [5] -[8]. In these papers, with the use of formal and rigorous homogenization techniques, multiscale reaction-diffusion systems modelling

sulphate corrosion were studied, for the case where microscopic fixed boundaries separate corroded and uncorroded parts of the material.

In [9] the formation and evolution of a mushy region was initially addressed. A mushy region in this case means that we have both uncorroded and corroded parts of the material coexisting during the process in an element volume of it and not having a distinct macroscopic interface separating the corroded and uncorroded parts of the material. This led to various macroscopic models for the process which where solved numerically.

The basic idea of [9] was to model the following, somehow idealized process. We assume that the bulk of the material under study, consists of uniform cells of square or cubical shape that are filled with calcite. The rest of the cell is a pore, void, filled with water and air. Inside the air and the water $H_2S$ is contained and under a chemical reaction in the water film, this is transformed to $H_2SO_4$ which next reacts with the calcite forming gypsum. The latter reaction is the one that causes the shrinkage of the calcite inside the cell and its outer surface can be modelled as a shrinking free boundary separating the remaining calcite with the gypsum formed and the pre-existing pore. Note that in some cases (see [9]) the reaction for the formation of $H_2SO_4$ is faster than the one forming gypsum and this fact can be used to simplify the analysis.

Although in [9] the problem for the microstructure was treated by assuming, in a specific way of how the moving boundary evolves. Namely it is taken that the moving boundary of the calcite has the form of a shrinking cycle at all times, intersecting the cell boundary of a cement volume element in a specific form (tangent or forming an angle).

In this paper the same essentially model is significantly improved by considering also the relevant equation describing the velocity of the moving boundary at each time which is coupled with the reaction - diffusion equation for the sulphate. This equation, which is a time dependent form of the Eikonal equation admits in some cases analytical solutions, the so called sandpile solutions and consequently we can result with a simplified version of the model, in the form of a non-local problem. In the cases that we don't have a useful analytical solution the problem can be solved numerically. With the use of an appropriate change in the time variable the numerical treatment of the full problem is further simplified and improved.

In the following of the paper in section 2 we proceed initially with a brief presentation of the model introduced in [1], which is the motivation of the present work. Also an appropriate nondimensionalization, as initially given in [9] is presented in order to get a convenient form of the reaction - diffusion equations.

In section 3 with the use of this scaled form of reaction diffusion equations, modelling concrete corrosion, and by applying the multiple scales method we derive from microstructure considerations a general averaged - type model for the macroscale. In these equations the order parameter is given by the solution of the Eikonal equation describing the boundary motion in a volume element of the material. Furthermore the analytical solutions of the Eikonal equation, for the cases that we have a specific form of the initial curve or surface surrounding the calcite, namely that of a square, cycle, cube or sphere, are presented. In these cases the model takes a simpler form of a non-local problem.

In section 4 the model in its various forms is treated numerically via a finite element method. When this is needed the Eikonal equation for the moving boundary is solved with the use of an upwind scheme either in the two or in the three dimensional case. Various numerical simulations are also presented.

Finally a discussion of the results of this paper and possible future work extensions are given in section 5.

## 2. Presentation of the Original Model

Initially we present briefly the original model that is the motivation and the basis of the more general models regarding concrete corrosion studied here.

In detail the governing chemical reactions describing the sewer pipes corrosion (see [1], [9]) are the following

$$\begin{aligned} 10\mathrm{H}^+ + \mathrm{SO}_4^{2-} + \text{org. matter} &\longrightarrow \mathrm{H_2S} + 4\mathrm{H_2O} + \text{oxidized org. matter} \\ \mathrm{H_2S} + 2\mathrm{O_2} &\xrightarrow{K_B} 2\mathrm{H}^+ + \mathrm{SO}_4^{2-} \\ 2\mathrm{H_2O} + \mathrm{H}^+ + \mathrm{SO}_4^{2-} + \mathrm{CaCO_3} &\xrightarrow{K_c} \mathrm{CaSO_4 \cdot 2H_2O} + \mathrm{HCO_3^-}. \end{aligned}$$

We denote by $u, v$ and $w$ the concentrations of $\mathrm{H_2S}$ in the gaseous phase (in ppmv), of $\mathrm{H_2S}$ in the liquid phase (in moles/volume) and of $\mathrm{SO}_4^{2-}$ (in moles/volume) respectively, i.e. $u := [\mathrm{H_2S}]_{\mathrm{g}}$, $v := [\mathrm{H_2S}]_{\mathrm{aq}}$ and $w := [\mathrm{SO}_4^{2-}]$, where $[\,\cdot\,]$ denotes the concentration, the subscript $g$ the gaseous phase, while the subscript $aq$ stands for water. Therefore the resulting set of equations that hold in the interior of the pores inside the concrete (see [1]), has the form

$$u_t = D_a u_{xx} - \frac{K_T A_S}{V_a}(K_{HS} u - v), \tag{2.1a}$$

$$v_t = D_w v_{xx} + \frac{K_T A_S}{V_w}(K_{HS} u - v) - K_B v, \tag{2.1b}$$

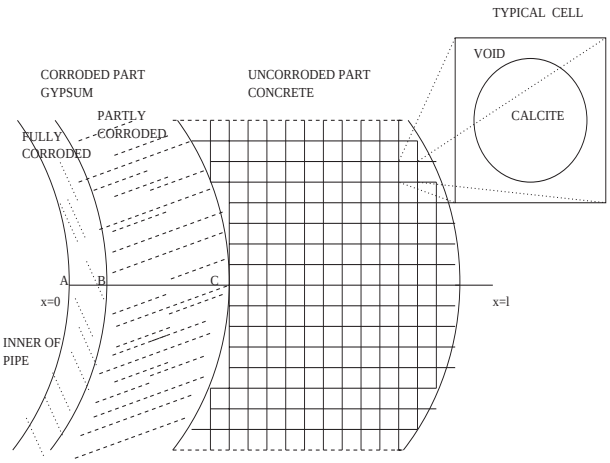


*Figure 1. Schematic representation of the wall of a sewer pipe under corrosion.*

$$w_t = D_H w_{xx} + K_B v. \tag{2.1c}$$

Indeed we have that $H_2S$ is exchanged between gaseous and liquid phase and this is expressed by the term $-(K_T A_S/V_a)(K_{HS}u - v)$, where $K_T$ is the mass transfer coefficient, $A_S$ is the surface area, $V_a$ is the air-filled effective porosity, i.e. the fraction of air filled pores in the material and $K_{HS}$ is the Henry's law constant.

In addition in the equation for $v$ we have a similar term $(K_T A_S/V_w)$ $(K_{HS}u - v)$ with $V_w$ being the water-filled effective porosity, i.e. the fraction of water filled pores in the material. Also the term $-K_B v$ expresses the bio-conversion of $H_2S$ with $K_B$ being the bio-conversion rate constant.

Moreover $D_a, D_w$ and $D_H$ are the relevant diffusion coefficients for $H_2S$ in the gaseous phase, for $H_2S$ in the liquid phase and for $SO_4^{2-}$ respectively.

A straight forward way to formulate the problem is to consider these equations in a domain representing a concrete wall (possible the inner part of a wall of a sewer pipe) which we consider for simplicity to be corroded in a one dimensional way. This can be seen in Figure 1 where we may assume that the point $C$ corresponds to a sharp interface separating fully corroded and uncorroded regions, moving to the right. In this setting (as in [1]) the area determined between the points A and C in the figure is supposed to be fully corroded and point B coincides with C. Note that in the setting considered later in section 3, where we assume the formation of a mushy region, we have a part that is fully corroded, between points A and B, an area that is partly corroded

between points B and C, i.e. the mushy region, and the uncorroded part right of the point C.

More specifically and returning to the setting described in [1], we may have that these equations apply for $x \in \Omega(t) = (0, s(t))$ where $x = 0$ stands for the left-end of the concrete wall, i.e. point A, and $s(t)$ for the point C in Figure 1. It is also reasonable to assume that the amount of the chemicals involved in the process ($H_2S$ in air and water and $SO_4^{2-}$ in the water) have constant concentration inside the pipe and also at the left end of the concrete segment. Thus we may impose Dirichlet boundary conditions of the form

$$u(0,t) = \lambda_1, \quad v(0,t) = \lambda_2, \quad w(0,t) = \lambda_3, \tag{2.2}$$

with $\lambda_1, \lambda_2, \lambda_3$ the given concentrations at $x = 0$. The right end $x = s(t)$ represents the corrosion front moving to the right as the process evolves. Neumann conditions should be applied for $u$ and $v$ and Robin conditions for $w$. The later comes from the fact that the flux of $w$ arriving at the interface is consumed by the chemical reaction transforming concrete into gypsum. Also the position of the moving boundary should be given by a kinetic condition, which has the form of the standard Stefan condition and we have

$$u_x(s(t),t) = 0, \;\; v_x(s(t),t) = 0, \;\; K_c\,(w(s(t),t)) + D_H w_x(s(t),t) = 0, \tag{2.3a}$$

$$\dot{s}(t) = \frac{K_c}{C_c} w, \tag{2.3b}$$

where $K_c$ is the dissolution rate constant (in length/time) and $C_c$ the alkalinity as calcium carbonate in concrete (in moles/volume). Note that alternatively, equation (2.3b) can be written also in the more common form $\dot{s}(t) = -(D_H/C_c)w_x$.

To summarize the chemistry of the process (see [1]), modelled by equations, (2.1), (2.2) and (2.3) as a macroscopic moving boundary problem, we have that $H_2S$ is created in the gaseous phase, due to bacteria, which next is transferred in the water phase as is indicated by the source term $(-(K_T A_S/V_a)(K_{HS}u - v))$, accounting of Henry's law in the equation of $u$ and $v$. Then $H_2S$ reacts with oxygen in the liquid phase, due to microorganisms catalysing the reaction, to produce $SO_4^{2-}$ and this is expressed by the source term in the equation for $v$ and $w$ $(\mp K_B v)$. Finally the produced $SO_4^{2-}$ reacts with calcite to produce gypsum and this is modelled by a Stefan condition in the boundary.

Since we have a significant planar propagation of the corrosion front away from corners (see [1]), the problem is set in its one dimensional form.

*Nondimensionalization.* We focus our attention to the system of equations (2.1), (2.2), (2.3) and we scale the problem by the use of appropriate constants. We scale $x$ with $l$, $y = x/l$ where $l$ is a typical length of the observed corrosion in a period of years i.e. an empirical estimation of the corrosion length in such a time period or a macroscopic length associated with the thickness of the concrete wall. We scale $u$, $v$, $w$ with $\lambda_1$, $\lambda_2$, $\lambda_3$ respectively and we have

$$U = \frac{u}{\lambda_1}, \quad V = \frac{v}{\lambda_2}, \quad W = \frac{w}{\lambda_3}, \quad S = \frac{s}{l}.$$

We set $\tau = t/t_0$ for $\tau$ being the dimensional variable and for $t_0$ a typical time which will be chosen in such a way so that the terms in the equation of the moving boundary are balanced. Thus we choose $t_0 = C_c l/(K_c \lambda_3)$.

Summarizing we have the system

$$\epsilon_1 \frac{\partial U}{\partial \tau} = \frac{\partial^2 U}{\partial y^2} - \mu_1 \left(\beta_1 U - V\right), \tag{2.4a}$$

$$\epsilon_2 \frac{\partial V}{\partial \tau} = \frac{\partial^2 V}{\partial y^2} + \mu_2 \left(\beta_1 U - V\right) - \beta_2 V, \tag{2.4b}$$

$$\epsilon_3 \frac{\partial W}{\partial \tau} = \frac{\partial^2 W}{\partial y^2} + \beta_3 V \tag{2.4c}$$

for $0 < y < S(\tau)$, with boundary conditions,

$$U(0,\tau) = 1, \qquad U_y(S(\tau),\tau) = 0, \tag{2.5a}$$

$$V(0,\tau) = 1, \qquad V_y(S(\tau),\tau) = 0, \tag{2.5b}$$

$$W(0,\tau) = 1, \qquad \gamma W_y(S(\tau),\tau) + W(S(\tau),\tau) = 0, \tag{2.5c}$$

the condition for the moving boundary,

$$\dot{S}(\tau) = W(S(\tau),\tau), \quad S(0) = S_a, \tag{2.6}$$

for $\tau > 0$, some $S_a > 0$ and the initial conditions

$$U(y,0) = 0, \quad V(y,0) = 0, \quad W(y,0) = 0, \quad 0 < y < S(0). \tag{2.7}$$

Here $\epsilon_1 = l^2/(D_a t_0)$, $\mu_1 = K_T A_s \lambda_2 l^2/(V_a \lambda_1 D_a)$ and $\beta_1 = K_{HS}\lambda_1/\lambda_2$ in the equation for $u$. Also $\epsilon_2 = l^2/(D_w t_0)$, $\mu_2 = K_T A_s l^2/(V_w D_w)$ and $\beta_2 = k_B l^2/D_w$ in the equation for $v$ and $\epsilon_3 = l^2/(D_H t_0)$, $\beta_3 = k_B \lambda_2 l^2/(D_H \lambda_3)$ in the equation for $w$. Moreover $\gamma = D_H/(l K_c)$.

Note that by choosing $t_0$ as the time scale of the fastest chemical reaction we result with the parameters $\epsilon$ having the form of Thiele - like modulus (or Damköhler numbers).

## 3. Mushy Region Model

As it is stated in [1], and initially considered in [9], it is worth considering a model for gypsum formation which allows gypsum and concrete to coexist at some volume element. This element may be specified as one cell, possible in the form of a square, containing a single pore, or as one having its length side of order similar to the radius of a cross-section of a typical pore.

To address this we assume that through the concrete and due to its porosity and the cracks existing in it, there is diffusion (dispersion) of $SO_4^{2-}$ which reacts with the concrete, i.e. the calcite, forming gypsum. The reaction takes place initially at the cracks' inner surface surrounding the pure solid calcite. Then gypsum is formed, having larger porosity than the concrete and thus new cracks are formed and diffusion takes place in the gypsum - void (containing no solid and filled with air and water) due to cracks area.

Based on this assumption, in the following we may take such an element in the microstructure, which is determined by the space between neighbouring cracks, to be corroded in such a way, amongst possible others, so that the corrosion evolves in two - dimensional or three - dimensional way.

More specifically, we initially study the problem in the microstructure which corresponds to a two or three dimensional geometry depending on how the structure of the material is assumed to be, i.e. in our case consisted by an infinite amount of identical cells in a form of squares or cubes (e.g. as the typical square cell in Figure 1). The reaction - diffusion equations for the chemicals involved in the process, hold inside the pores (void) in these cells which are filled with air and water containing $H_2S$ and $SO_4^{2-}$. For convenience later in the asymptotic analysis we may also allow flow, but no reaction, inside the calcite core of the cell, due to minor pores of small size (negligible) compared with the cell size. Therefore in the microstructure consideration we apply the two (for square cells) or three (for cubic cells) dimensional form of these equations. A one - dimensional consideration for the microstructure have been also studied in [9] but is not of further interest. After applying the averaging procedure we get the equations for the macroscale which in general account for the three dimensional space. Depending now on the specific geometry in the macroscale, i.e. if we have a plate or a rod under corrosion, we may simplify the setting of the macroscopic equations and reduce them into its two or one - dimensional form. This is actually done here, for the sewer pipe model where the derived equation are reduced to its one-dimensional form since as it is already

mentioned, in practice we have significant propagation of the corrosion in a one - dimensional way.

Therefore in the following we will consider a square or a cubic cell, say $\Omega$, with boundary $\partial\Omega = \Gamma_e$, which initially contains pure calcite occupying the domain $\Omega_c$ with its boundary $\partial\Omega_c = \Gamma_c$ separating it initially from the void space. Namely we take the pore, inside the cell, to be specified by the boundaries $\Gamma_e$ and $\Gamma_c$ and its domain before the corrosion process starts is $\Omega_v = \Omega \setminus \Omega_c$ (see Figure 2(a)). The area of $\Omega_v$ should be such that $|\Omega_v|/|\Omega| = \phi_c$ for $\phi_c$ being the porosity of the cement. As corrosion evolves and gypsum is formed the boundary $\Gamma_c$ now separates pure calcite from the gypsum and void parts of the rest of the element. We denote the gypsum-void part of the element by $\Omega_g$ and we have $\Omega = \Omega_g \cup \Omega_c$ (see Figure 2(b)). Note that at $t = 0$, $\Omega_g(0) = \Omega_v$. This process continues until the transformation of the calcite to gypsum is completed and have $\Omega = \Omega_g$, $\Gamma_c = \emptyset$ (see Figure 2(c)).

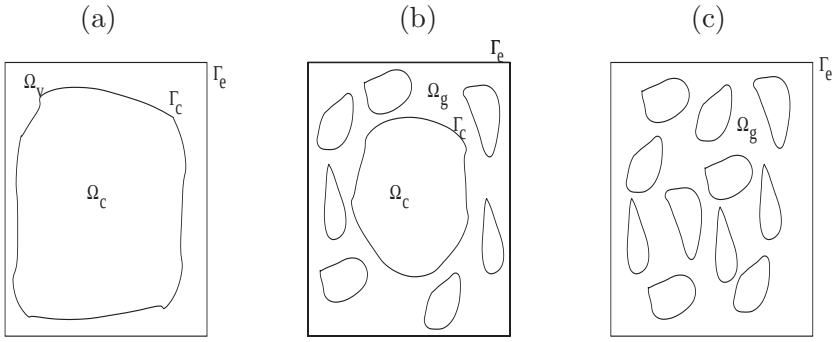


*Figure 2. Schematic representation of the corrosion of a concrete element.*

The above image may be very well inverted and we may consider having the pore contained inside the element. In such a case the calcite should occupy the area contained between the boundaries $\Gamma_e$ and $\Gamma_c$. Then as the process evolves $\Gamma_c$ is approaching $\Gamma_e$, the calcite area decreases and at the end of the process we have $\Gamma_c = \Gamma_e$. This consideration might be more appropriate, and more realistic in our case, if we consider a cross section of a pore contained in calcite.

Furthermore these configurations may be easily adapted in the three dimensional space where the cement element - cell may be a cube now and the $\Gamma's$ two dimensional surfaces.

In addition in each case the porosity $\phi$ of the element should be given at each time $t$, by the relation

$$\phi = (\phi_g - \phi_c)\frac{|\Omega_g(t)| - |\Omega_g(0)|}{|\Omega| - |\Omega_g(0)|} + \phi_c,$$

where $\phi_g$ is the porosity of the gypsum, giving $\phi = \phi_c$ for $t = 0$ and $\phi = \phi_g$ when $\Omega_g = \Omega$.

Finally due to the fact that the porosity of the gypsum is larger than that of the cement we have volume expansion. However including this characteristic in the model complicates further the analysis. To keep things simple, as in [9], we assume in the following that this volume expansion is negligible, compared with the length scale of the wall thickness, and hence will not be further considered.

### 3.1. Derivation of the Model

We assume that $SO_4^{2-}$ diffuses in a two dimensional (or three dimensional) way in a volume element and its concentration satisfies the dimensionless equation

$$\varepsilon W_\tau = \Delta W + f, \tag{3.1}$$

with $\varepsilon$ being a dimensionless parameter and $f$ being a source term, possibly non-linear, modelling the production or supply of $SO_4^{2-}$ in the system, which then reacts with the calcite. For example in the case of the sewer pipe corrosion model, $f$ is equal to $\beta_3 V(y, \tau)$. In another case such as monument corrosion etc, $f$ may have a different form, but still expressing the supply of the system with $SO_4^{2-}$. Moreover $W = W(y, \tau)$ and in general $y \in \mathbb{R}^n$, $n = 1, 2, 3$ depending the macroscopic geometry of the material under consideration.

Instead of studying the full system of equations (2.4) we focus in equation (3.1), which is a more general form of equation (2.4c), for two reasons. The first is to give some generality in the analysis that follows i.e. to be able to account for different systems as this is expressed by the possible forms of the function $f$. The second reason is to simplify the presentation of the analysis since the process presented in the following can be applied in exactly the same way for the equations (2.4a) and (2.4b) in the sewer pipe corrosion problem.

In addition the boundary condition at the interface $\Gamma_c$ of the corroded - uncorroded material will be

$$\gamma \left[\frac{\partial W}{\partial n}\right] + W = 0, \quad y \in \Gamma_c, \tag{3.2}$$

where $n$ is the outward normal vector at a point of the moving boundary $\Gamma_c$, $[\cdot]$ denotes the flow jump at $\Gamma_c$ and the dimensionless constant

$\gamma$ can be written as $\gamma = \gamma_m/\delta$, where $\delta$ is the ratio of the microscopic and macroscopic length scales.

Furthermore the motion of the boundary is given by the standard Stefan condition.

$$-\gamma_m \left[\frac{\partial W}{\partial n}\right] = \mathsf{V}, \quad y \in \Gamma_c, \tag{3.3}$$

where $\mathsf{V}$ is the speed of the moving boundary.

The latter form of the equation in the boundary, comes from the fact that we want, in the microscopic scale, the speed of the moving boundary $\Gamma_c$ to be proportional to the rate of reaction. This is apparent later and eventually in equation (3.10d). We recall also that the time scale $t_0$, with $\tau = t/t_0$, and the length scale $l$, with $y = x/l$, can be chosen appropriately so that to obtain the Stefan condition into the above form and thus to be able to "see" the motion of the boundary in the microscale (the same essentially analysis is also followed initially in [10] and also in [9]).

Regarding the geometry of the porous medium we assume that initially it consists of a collection of pores, i.e voids containing cement. A closed curve, $\Gamma_c$, assumed to be at least piecewise smooth, is the boundary of the calcite area. This curve might have various shapes. Here initially we consider three cases for the shape of these closed curves : (1) a rectangular (2) a circle (3) an ellipse or more generally a Lamé curve (e.g. see [11], ch. 2).

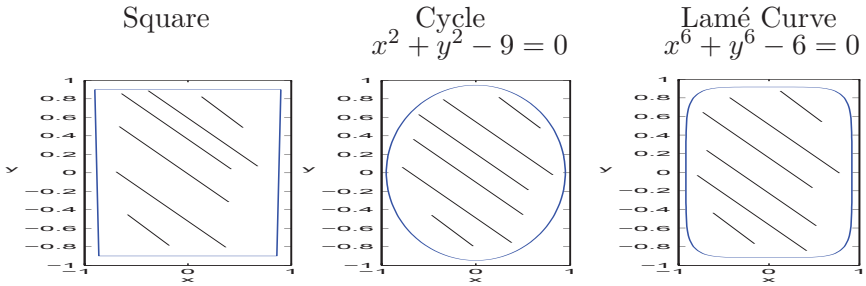


*Figure 3. Possible initial boundaries $\Gamma_c$ surrounding pure calcite.*

In any case the square cell is assumed to have a side of length $2d$ where $d$ can be taken to be of order of an average distance between two pores inside the material or the average diameter of a pore inside it. This distance can be used as a characteristic length in the microscopic scale. Also as a scale for the macroscopic problem, say $l$ can be taken for example the width of a concrete slab or the thickness of a wall etc., whose corrosion is being studied.

In addition we have that $\Gamma_c$ can be described by some function $\mathsf{s} = \mathsf{s}(y, \tau)$ ($\mathsf{s} = s/l$ for $s$ the dimensional boundary position) giving the position of the boundary at each time.

In the following we apply the methodology described in [10], [12] and [9]. We consider two spatial scales for the problem, the macroscopic length scale represented by the variable $y$ and a microscopic length scale represented by the variable $z$. As it is already mentioned $l$ is the typical macroscopic length scale, and $d$ is the microscopic length scale. We take $d \ll l$ and their ratio is $\delta = d/l \ll 1$.

Note that this small parameter $\delta$ corresponds to the ratio of the micro and macro length scales, while the parameter $\varepsilon$ in equation (3.1), which in cases might be small, is the ratio of the time scales, of the diffusion of $SO_4^{2-}$ and of the reaction forming gypsum ($\varepsilon = (l^2/D_H)/t_0$ for $t_0$ being a characteristic time scale of the reaction). For the following analysis to hold we will assume that even for the case that we have $\varepsilon \ll 1$ the condition $1 \gg \varepsilon \gg \delta$ holds.

As a next step, we take

$$W = W(y, z, \tau),$$

where, for $x$ being the dimensional original distance, $x = ly$ and $x = dz$ with $\delta = d/l \ll 1$. The position of the boundary $s$ is scaled with $d$ and we take $S = s/d$ $(= (l/d)\mathsf{s} = (1/\delta)\mathsf{s})$. We also assume that $\gamma_m = O(1)$.

The multiple scales approach (see [13]) gives instead for the spatial derivative $\nabla_y W$ at the point $(y, z, t)$ the expression

$$\nabla_y W + \frac{1}{\delta}\nabla_z W.$$

Rescaling also with $d$ the speed of the boundary $\mathsf{V}$, will give $\mathsf{V} = \delta\mathcal{V}$, where $\mathcal{V}$ is the new dimensionless variable for the speed (Dimensional boundary speed $= \mathsf{V}\, l/t_0 = \mathcal{V}\, d/t_0$, or $\mathsf{V} = \delta\mathcal{V}$). This also implies that $\mathcal{V} = W$ on $\Gamma_c$.

More precisely for $\mathcal{S}$ being the function representing the position of the boundary in the form $\mathcal{S}(y, z, \tau) = 0$, ( $\mathcal{S}(y, z, \tau) = z_2 - S(y, z_1, \tau) = 0$), we have that the rescaled speed of the boundary $\mathcal{V}$, has the form

$$\mathcal{V} = \frac{\partial \mathcal{S}}{\partial \tau}\frac{1}{|\nabla_z \mathcal{S} + \delta\nabla_y \mathcal{S}|},$$

given that in place of $|\nabla \mathsf{s}(y, \tau)|$ we have $|(1/\delta)\nabla_z \mathsf{s}(y, z, \tau) + \nabla_y \mathsf{s}(y, z, \tau)| = |\delta(1/\delta)\nabla_z \mathcal{S}(y, z, \tau) + \delta\nabla_y \mathcal{S}(y, z, \tau)|$. Application of the multiple scales method implies

$$\varepsilon W_\tau = \frac{1}{\delta^2}\nabla_z^2 W + \frac{2}{\delta}\nabla_y \nabla_z W + \nabla_y^2 W + f.$$

Regarding the Stefan condition, (3.3), we have

$$\delta\mathcal{V}=\delta\frac{\partial\mathcal{S}}{\partial\tau}\frac{1}{|\nabla_z\mathcal{S}+\delta\nabla_y\mathcal{S}|}=-\gamma_m\frac{1}{\delta}\,n\cdot[\nabla_z W+\delta\nabla_y W]\,,$$

and also at the boundary

$$\gamma_m\,n\cdot[\nabla_z W+\delta\nabla_y W]+\delta^2 W=0.$$

The square cell has side of scaled length 2. Also $\Omega:=[-1,\,1]\times[-1,\,1]$, with $z\in\Omega$ and in its boundary symmetry conditions should be applied for the variable $W$. Therefore we must have periodic conditions at the sides of the square boundary ([9],[10]) resulting in a condition of the following form :

$$n\cdot\nabla W|_{\partial\Omega}=0.$$

This comes from the fact that, for example for a 2-dimensional square cell, these periodic conditions have the following form:

$$\begin{aligned}
W(y,z_1,-1,\tau)&=W(y,z_1,1,\tau),\quad -1\le z_1\le 1,\\
W(y,-1,z_2,\tau)&=W(y,1,z_2,\tau),\quad -1\le z_2\le 1,\\
W_{z_2}(y,z_1,-1,\tau)&=W_{z_2}(y,z_1,1,\tau),\quad -1\le z_1\le 1,\\
W_{z_1}(y,-1,z_2,\tau)&=W_{z_1}(y,1,z_2,\tau),\quad -1\le z_2\le 1.
\end{aligned}$$

For a symmetric cell also we have $W(y,z_1,z_2,\tau)=W(y,z_1,-z_2,\tau)=W(y,-z_1,z_2,\tau)$ and summarizing the above relations we obtain $\partial W/\partial n=0$ in $\partial\Omega$. More specifically we consider an infinite set of square cells, inside the material indistinguishable between them and therefore the condition $\partial W/\partial n=0$ should be applied in the outer boundary of them. This is the reason why in our analysis we focus our attention in one cell occupying a region $\Omega$ with boundary $\partial\Omega$.

In the following we proceed with a formal asymptotic expansion for $W$ and $S$. The equations for $W$, by assuming that $W\sim W_0+\delta W_1+\ldots$, $f=f_0+\delta f_1+\ldots$ take the form

$$\begin{aligned}
\varepsilon W_{0\tau}+\delta\varepsilon W_{1\tau}+\delta^2\varepsilon W_{2\tau}+\ldots\;=\;&\frac{1}{\delta^2}\nabla_z^2W_0+\frac{2}{\delta}\nabla_z\nabla_yW_0+\nabla_y^2W_0+f_0\\
&+\frac{1}{\delta}\nabla_z^2W_1+2\nabla_z\nabla_yW_1+\delta\nabla_y^2W_1+\delta f_1\\
&+\nabla_z^2W_2+2\delta\nabla_z\nabla_yW_2+\delta^2\nabla_y^2W_2+\delta^2f_2\\
&+\delta\nabla_z^2W_3+2\delta^2\nabla_z\nabla_yW_3+\ldots.
\end{aligned}$$

Also at the points $(y,z,\tau)$ with $z=(z_1,z_2)\in\Gamma_c$, we have for $\mathcal{S}=\mathcal{S}_0+\delta\mathcal{S}_1+\ldots$, and $|\nabla_z\mathcal{S}+\delta\nabla_y\mathcal{S}|=|\nabla_z\mathcal{S}_0+\delta\nabla_y\mathcal{S}_0+\delta\nabla_z\mathcal{S}_1+\ldots|$,

that

$$\frac{\partial \mathcal{S}_0}{\partial \tau}\frac{1}{|\nabla_z \mathcal{S}_0|} = -\gamma_m\, n\cdot\left[\tfrac{1}{\delta^2}\nabla_z W_0 + \tfrac{1}{\delta}\nabla_y W_0 + \tfrac{1}{\delta}\nabla_z W_1 + \nabla_y W_1 + \nabla_z W_2 + \ldots\right],$$
$$W_0 + \gamma_m\, n\cdot\left[\tfrac{1}{\delta^2}\nabla_z W_0 + \tfrac{1}{\delta}\nabla_y W_0 + \tfrac{1}{\delta}\nabla_z W_1 + \nabla_y W_1 + \nabla_z W_2\right] + \ldots = 0.$$

Then for order $O(1/\delta^2)$ terms we have $\nabla_z^2 W_0 = 0$. By the conditions at the moving boundary $\Gamma_c$, i.e. at $z = S$ we get $n\cdot\nabla_z W_0 = 0$. In addition at the cell boundary, $\partial\Omega$ we have again $n\cdot\nabla_z W_0 = 0$. By these equations and a direct application of the maximum principle we deduce that $W_0 = W_0(y,\tau)$.

For order $O(1/\delta)$ terms we have $2\nabla_z\nabla_y W_0 + \nabla_z^2 W_1 = 0$, or $\nabla_z^2 W_1 = 0$ due to the fact that $W_0 = W_0(y,\tau)$. In addition at the boundary $z_2 = S$ we have $n\cdot[\nabla_y W_0 + \nabla_z W_1] = 0$, while at the cell boundary $\partial\Omega$, we have similarly $n\cdot[\nabla_y W_0 + \nabla_z W_1] = 0$. Thus as for the $O(1/\delta^2)$ terms, by using the same arguments, the fact that $n\cdot\nabla_y W_0$ is constant over the boundary because $W_0 = W_0(y)$, and that the jump in the flux $[n\cdot\nabla_y W_0] = 0$, we deduce that $W_1 = W_1(y,\tau)$.

Then for $O(1)$ terms, given that $\nabla_z W_1 = 0$, we have

$$\varepsilon W_{0\tau} = \nabla_y^2 W_0 + \nabla_z^2 W_2 + f_0, \tag{3.4}$$

while at the boundary,

$$\frac{\partial \mathcal{S}_0}{\partial \tau}\frac{1}{|\nabla_z \mathcal{S}_0|} = -\gamma_m\, n\cdot[\nabla_y W_1 + \nabla_z W_2]\,.$$

We proceed by averaging the field equation, (3.4), over the whole domain occupied by the pore-gypsum area, say $\Omega_g$ (since the porosity inside the calcite core of the cell is taken to be negligible). Averaging can be done by integrating both sides with respect to $z$ over $\Omega_g$. In this way we can eliminate the $z$-dependence from the equations and obtain an equation depending only in $y$ and $\tau$, describing the phenomenon at the macroscopic scale.

Due to the fact that the condition $n\cdot\nabla W = 0$ in $\partial\Omega$ is applied to each of the indistinguishable cells, averaging the equation for $W_0$ yields :

$$\int_{\Omega_g}\left[\varepsilon W_{0\tau} - \nabla_y^2 W_0 - f_0\right] dz = \int_{\Omega_g}\nabla_z^2 W_2 dz = \int_{\Gamma_c\cup\Gamma_e} n\cdot\nabla_z W_2 dz,$$

or

$$\phi_g A(y,\tau)\left[\varepsilon W_{0\tau} - \nabla_y^2 W_0 - f_0\right] = \int_{\Gamma_c} n\cdot\nabla_z W_2 dz + \int_{\Gamma_e} n\cdot\nabla_z W_2 dz,$$

where $A(y,\tau)$ is the area of the cell occupied by the gypsum, i.e $A(y,\tau) = \int_{\Omega_g} dz$.

Note that the symmetry conditions at the cell boundary $\partial\Omega$ give $\int_{\Gamma_e} n\cdot\nabla_z W_2 dz = 0$ while similarly we also have $\int_{\Gamma_c\cup\Gamma_e} n\cdot\nabla_y W_1 dz = 0$. Additionally we have that $\int_{\Gamma_c\bigcap\Gamma_e} n\cdot\nabla_z W_2 dz = 0$.

Next we denote by $F(S)$ the source term appearing in the equation of $W_0$, which, due to the expansion of the Stefan and the Robin conditions at the boundary, takes the form

$$F(S) := \int_{\Gamma_c\setminus(\Gamma_c\bigcap\Gamma_e)} n\cdot\nabla_z W_2 dz = \frac{1}{\gamma_m} W_0 \int_{\Gamma_s} dz,$$

for $\Gamma_s = \Gamma_c\setminus(\Gamma_c\bigcap\Gamma_e)$. Moreover the length of this part of the moving boundary, $\Gamma_s$ will be denoted by $L = \int_{\Gamma_s} dz$. Thus the final set of equations that are derived by this process, modelling corrosion in a macroscopic scale is

$$\varepsilon W_{0\tau} - \nabla_y^2 W_0 - f_0 \;=\; -\frac{1}{\gamma_m\phi_g} W_0 \frac{L(y,\tau)}{A(y,\tau)}, \tag{3.5}$$

$$\frac{\partial\mathcal{S}_0}{\partial\tau}\frac{1}{|\nabla_z\mathcal{S}_0|} \;=\; W_0. \tag{3.6}$$

Also by the fact that to first order terms we have $\mathcal{S} = z_2 - S(y,z_1,\tau) \simeq \mathcal{S}_0$ we get

$$L(y,\tau) = \textstyle\int_{\Gamma_s} dz = 4\int_0^1 \sqrt{1+\left(\frac{\partial S}{\partial z_1}\right)} dz_1,$$

$$A(y,\tau) = 4\left[1 - \textstyle\int_0^1 S(y,z_1,\tau) dz_1\right].$$

Note that the $(y,\tau)$ dependence of $L$ and $A$ comes from the form of $S = S(y,z_1,\tau)$ as this being the solution of equation (3.6). Also $A(y,\tau)$ due to symmetry, can be calculated by taking four times the area in the square $[0,1]\times[0,1]$. This is used also later in the numerical treatment of the problem. In addition the porosity at the point $y$ at time $\tau$ will be

$$\phi(y,\tau) = (\phi_g - \phi_c)\frac{A(y,\tau) - A(y,0)}{|\Omega| - A(y,0)} + \phi_c, \tag{3.7}$$

with $|\Omega| = 4$ in this case, for a two-dimensional square cell.

These equations, (3.5) and (3.6), account for the actual concentration $W$ of $\mathrm{SO}_4^{2-}$ while the effective concentration $\bar{W}$ is given by $\bar{W} = \phi W$. This describes the fact that $\mathrm{SO}_4^{2-}$ diffuses actually in the pores of the material and not in the whole domain of it. Moreover considering the case that we study a slab of concrete being corroded due to the presence of $\mathrm{SO}_4^{2-}$ at the one end of it, we may proceed with

an one dimensional setting of the derived equations and take $y \in [0,1]$. Therefore the actual concentration $\bar{W}$ at the boundary $y = 0$, after appropriate scalling can be set to be $\bar{W}(0,\tau) = W(0,\tau)\phi(0,\tau) = 1$ and therefore we have

$$W(0,\tau) = \frac{1}{\phi(0,\tau)}. \tag{3.8}$$

At the point $y = 1$ we assume that we have Neumann conditions due to symmetry or due to the fact that there is some kind of insulation at this point (e.g. having some material for $y \geq 1$, that it is not penetrated and corroded by sulphate can allow us to take a zero flux condition at this point). Therefore, in our case, we have $\bar{W}_y(1,\tau) = 0$ and consequently $W_y(1,\tau)\phi(1,\tau) + \phi_y(1,\tau)W(1,\tau) = 0$ or

$$W_y(1,\tau) + \frac{\phi_y(1,\tau)}{\phi(1,\tau)}W(1,\tau) = 0. \tag{3.9}$$

These conditions, (3.8) and (3.9), correspond to the setting applied for the study of the sewer pipes corrosion problem as in [9]. Other boundary conditions may very well posed and easily adapted to the model.

Summarizing, the equations derived, for the case that we consider one dimension in the macroscale, and by dropping the subscripts in the notation for $W$ and $\mathcal{S}$ since $W \simeq W_0$, $\mathcal{S} \simeq \mathcal{S}_0$, we have

$$\varepsilon W_\tau - W_{yy} - f_0(y,\tau) = -\frac{1}{\gamma_m \phi_g} W \frac{L(y,\tau)}{A(y,\tau)}, \quad 0 < y < 1, \quad \tau \geq 0 \tag{3.10a}$$

$$W(0,\tau) = \frac{1}{\phi(0,\tau)}, \quad W_y(1,\tau) + \frac{\phi_y(1,\tau)}{\phi(1,\tau)}W(1,\tau) = 0, \tag{3.10b}$$

$$W(y,\tau) = W_a(y), \tag{3.10c}$$

$$-\frac{\partial S}{\partial \tau}\frac{1}{\sqrt{1 + \left(\frac{\partial S}{\partial z_1}\right)^2}} = W(y,\tau), \quad 0 < z_1 < 1, \quad \tau \geq 0, \tag{3.10d}$$

$$S(y,z_1,0) = S_a(z_1), \quad \frac{\partial S}{\partial z_1}(y,0,\tau) = 0, \tag{3.10e}$$

$$\phi(y,\tau) = (\phi_g - \phi_c)\frac{A(y,\tau) - A(y,0)}{4 - A(y,0)} + \phi_c, \tag{3.10f}$$

$$L(y,\tau) = 4\int_{S(y,z_1,\tau)} dz_{\Gamma_s}, \quad A(y,\tau) = 4\left[1 - \int_0^1 S(y,z_1,\tau)dz_1\right]. \tag{3.10g}$$

Here $W_a$ is the initial condition for $W$ and a natural choice to make is to take $W_a = 0$. Also $S_a$ is the initial position of the moving boundary, applied to all the cells inside the material, assumed to be independent of $y$ while for $\tau > 0$ its position is given by the points $(z_1, z_2)$ for which we have $z_2 = S(y, z_1, \tau)$.

This problem for $W$, $S$ can be solved numerically as it will be presented in the next section. In order to simplify things and not to solve simultaneously the equations for $W$ and $S$ we may use an appropriate change of the time variable.

More specifically, we focus on the equation for $S = S(y, z_1, \tau)$, where we have

$$-\frac{\partial S}{\partial \tau} = W(y,\tau)\sqrt{1+\left(\frac{\partial S}{\partial z_1}\right)^2},\ S(y,z_1,0) = S_a(z_1),\ \frac{\partial S}{\partial z_1}(y,0,\tau) = 0$$

and we set

$$\frac{\partial S}{\partial \tau} = \frac{\partial S}{\partial \sigma}\frac{\partial \sigma}{\partial \tau},$$

for $\sigma$ a new time variable. Thus we obtain

$$-\frac{\partial S}{\partial \sigma}\frac{\partial \sigma}{\partial \tau} = W(y,\tau)\sqrt{1+\left(\frac{\partial S}{\partial z_1}\right)^2},\ S(y,z_1,0) = S_a(z_1),\ \frac{\partial S}{\partial z_1}(y,0,\tau) = 0.$$

In order to simplify the problem we set $\partial\sigma/\partial\tau = W(y,\tau)$ or

$$\sigma = \sigma(\tau) = \int_0^\tau W(y,\tau')d\tau'.$$

Therefore we obtain for $S = S(z_1, \sigma)$,

$$-\frac{\partial S}{\partial \sigma} = \sqrt{1+\left(\frac{\partial S}{\partial z_1}\right)^2}, \quad 0 < z_1 < 1, \quad \sigma \geq 0 \tag{3.11a}$$

$$S(z_1, 0) = S_a(z_1), \quad S_{z_1}(0,\sigma) = 0. \tag{3.11b}$$

This is a form of the Eikonal equation $(\partial S/\partial\sigma)^2 - (\partial S/\partial z_1)^2 = 1$, for $S = S(z_1, \sigma)$.

At this point we have to emphasize the fact that through out the domain of the material under study we have assumed that all the cell elements are of the same form and in all of them the boundary separating initially the pure calcite from the pore is always $S_a = S_a(z_1)$ independent of $y$. Note also that in general we can have different types of cells, i.e. triangles, hexagonal, other type of identical polygons etc. (e.g. see [12]) but then more complications would arise in the analysis, which should be modified accordingly. In our case and for certain

choices of the initial conditions $S(y, z_1, 0) = S_a(z_1)$ we may have, simple enough ([14],[15]), analytical solutions for $S$ and consequently obtain a simpler form of the $W$ - problem.

### 3.2. Sandpile Solutions

*Square Segment.* We will consider the case that the calcite segment is of a square form, of side say $2L_0$, contained in a square cell with side of length 2. This corresponds to the following equation.

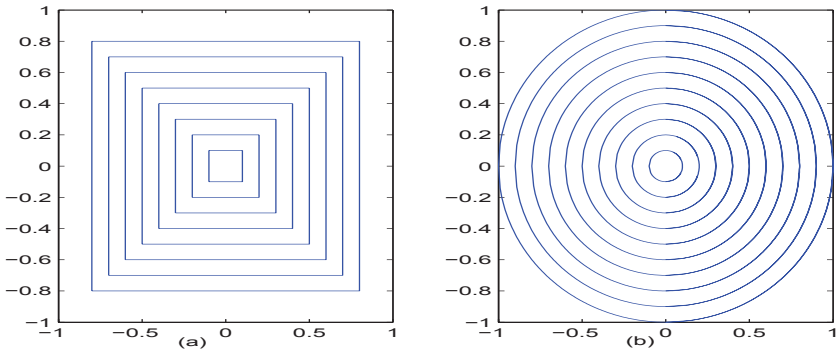


*Figure 4. Form of sandpile solutions in the case of the initial curve being (a) a square, (b) a cycle.*

$$-\frac{\partial S}{\partial \sigma} = \sqrt{1 + \left(\frac{\partial S}{\partial z_1}\right)^2}, \quad 0 < z_1 < 1, \quad \sigma \geq 0, \tag{3.12}$$
$$S(z_1, 0) = L_0, \quad \frac{\partial S}{\partial z_1}(0, \sigma) = 0.$$

The length of the square side $2L_0$ should be such that $(4 - (2L_0)^2)/4 = \phi_c$, and therefore $L_0 = \sqrt{1 - \phi_c}$.

This equation, (3.12), can be solved following the methodology for solution of quasilinear first order partial differential equations as presented e.g. in [14].

We set $p = S_{z_1}$, $q = S_\sigma$ and equation, (3.12), takes the form $G(p, q) = q^2 - p^2 - 1 = 0$. The relevant Charpit's equations are

$$\dot{z_1} = \frac{\partial G}{\partial p}, \quad \dot{\sigma} = \frac{\partial G}{\partial q}, \quad \dot{S} = p\frac{\partial G}{\partial p} + q\frac{\partial G}{\partial q},$$
$$\dot{p} = -\frac{\partial G}{\partial z_1} - p\frac{\partial G}{\partial S}, \quad \dot{q} = -\frac{\partial G}{\partial \sigma} - q\frac{\partial G}{\partial S},$$

or finally $\dot{z_{1s}} = G_p$, $\dot{\sigma} = G_q$, $\dot{S} = pG_p + qG_q$, $\dot{p} = \dot{q} = 0$. Thus $p = p_0(\xi)$, $q = q_0(\xi)$. The ray equations will be $z_1 = z_{10} + t_s\, G_p|_0$, $\sigma = \sigma_0 + t_s\, G_q|_0$, $S = S_0 + t_s\, (pG_p + qG_q)|_0$. The initial curve is such

that $p|_{z_1=0} = p_0 = 0$ with $q_0^2 - p_0^2 = 1$ or $q_0^2 = 1$ and $q = \pm 1$. Also $G_p = -2p$, $G_p|_0 = -2p_0 = 0$, $G_q|_0 = -2q_0 = \pm 2$ and $z_1 = z_{10}$, $\sigma = \sigma_0 + 2t_s$, $S = S_0 + t_s(-2q^2 + 2p^2) = S_0 + 2t_s$. Thus $2t_s = S - S_0$ and $\sigma = \sigma_0 \pm (S - S_0)$ or $S = \pm(\sigma - \sigma_0) + S_0$. For $\sigma_0 = 0$ we have $S_0 = L_0$ and $S = L_0 \pm \sigma$. By the initial equation we know that $S$ is decreasing with time and we finally obtain

$$S(z_1, \sigma) = L_0 - \sigma.$$

By the symmetry of the square element, we need at $S = z_1$, the free boundaries to intersect and thus we have $S = L_0 - \sigma$ for $0 \leq z_1 \leq L_0 - \sigma$. The moving boundary ceases to exist for $\sigma = 1$ where then the whole of the square element has been transformed to gypsum. Returning to the original time variable $\tau$ we obtain

$$S(y, z_1, \tau) = L_0 - \int_0^\tau W(y, \tau')d\tau'.$$

Consequently, for each time $\tau$ for a point $y$ we have

$$\begin{aligned} L(y,\tau) &= 8\,(L_0 - \sigma) = 8\left[L_0 - \int_0^\tau W(y,\tau')d\tau'\right], \\ A(y,\tau) &= 4 - 4\,(L_0 - \sigma)^2 = 4 - 4\left[L_0 - \int_0^\tau W(y,\tau')d\tau'\right]^2 \end{aligned}$$

and the equation for $W$ takes the form of a non-local problem

$$\varepsilon W_\tau = W_{yy} + f_0 - \frac{1}{\gamma_m \phi_g} W \frac{8\left[L_0 - \int_0^\tau W(y,\tau')d\tau'\right]}{\left[4 - 4\left(L_0 - \int_0^\tau W(y,\tau')d\tau'\right)^2\right]}, \quad \text{(3.13a)}$$

$$W(0,\tau) = \frac{1}{\phi(0,\tau)}, \qquad W_y(1,\tau) + \frac{\phi_y(1,\tau)}{\phi(1,\tau)} W(1,\tau) = 0, \quad \text{(3.13b)}$$

$$W(y,\tau) = W_a(y), \quad \text{(3.13c)}$$

for $0 < y < 1$, $\tau \geq 0$.

*Cyclical Segment.* In that case we assume that initially in a square cell we have a circular cement segment of radius $R_0$ such that $(4 - \pi R_0^2)/4 = \phi_c$, or $R_0 = 2\left((1 - \phi_c)/\pi\right)^{\frac{1}{2}}$.

Again we have the Eikonal equation

$$-\frac{\partial S}{\partial \sigma} = \sqrt{1 + \left(\frac{\partial S}{\partial z_1}\right)^2}, \quad 0 < z_1 < 1, \quad \sigma \geq 0,$$

$$S(z_1, 0) = \sqrt{R_0^2 - z_1^2}, \quad 0 \leq z_1 \leq 1, \quad S_{z_1}(0, \sigma) = 0, \quad \sigma \geq 0.$$

The solution can be obtained as in the previous paragraph or by assuming that the solution has a specific form. More precisely, for the latter case, we seek solutions of the form $S = \sqrt{g^2(\sigma) - z_1^2}$ with $g(0) = R_0$. We have $S_{z_1} = -z_1/\sqrt{g^2(\sigma) - z_1^2}$, $S_\sigma = -g'(\sigma)/\sqrt{g^2(\sigma) - z_1^2}$ and the condition $S_\sigma^2 - S_{z_1}^2 = 1$ gives $g^2(\sigma)g'^2(\sigma)/\left(g^2(\sigma) - z_1^2\right) - z_1^2/\left(g^2(\sigma) - z_1^2\right) = 1$ or $g'^2(\sigma) = 1$ and consequently, due to the fact that we must have $g' < 0$, $g'(\sigma) = -1$ or $g(\sigma) = R_0 - \sigma$.

Thus $S(z_1, \sigma) = \sqrt{(R_0^2 - \sigma)^2 - z_1^2}$, for $(R_0^2 - \sigma)^2 - z_1^2 > 0$ or $z_1 < R_0 - \sigma$ and $g = 0$ for $\sigma = R_0$. We recall that $\sigma = \int_0^\tau W(y, \tau')d\tau'$ and

$$S(y, z_1, \tau) = \left[\left(R_0 - \int_0^\tau W(y, \tau')d\tau'\right)^2 - z_1^2\right]^{\frac{1}{2}},$$

for $z_1 < R_0 - \sigma = R_0 - \int_0^\tau W(y, \tau')d\tau'$. The radius of the circle is $R(y, \tau) = R_0 - \int_0^\tau W(y, \tau')d\tau'$ at the point $(y, \tau)$ and therefore we have

$$\begin{aligned} L(y, \tau) &= 2\pi\left[R_0 - \int_0^\tau W(y, \tau')d\tau'\right], \\ A(y, \tau) &= \left[4 - \pi\left(R_0 - \int_0^\tau W(y, \tau')d\tau'\right)^2\right], \end{aligned}$$

while the macroscopic problem takes the form

$$\varepsilon W_\tau = W_{yy} + f_0 - \frac{1}{\gamma_m \phi_g} W \frac{2\pi\left[R_0 - \int_0^\tau W(y, \tau')d\tau'\right]}{\left[4 - \pi\left(R_0 - \int_0^\tau W(y, \tau')d\tau'\right)^2\right]}, \quad (3.14a)$$

$$W(0, \tau) = \frac{1}{\phi(0, \tau)}, \qquad W_y(1, \tau) + \frac{\phi_y(1, \tau)}{\phi(1, \tau)} W(1, \tau) = 0, \quad (3.14b)$$

$$W(y, \tau) = W_a(y), \quad (3.14c)$$

for $0 < y < 1$, $\tau \geq 0$.

These solutions can be generalized for the case of three dimensional elements and more specifically for cubic and spherical calcite segments and obtain again a simpler formulation of the problem.

*Cubic Segment.* In case that we have a cubic element of edge 2 we take $z = (z_1, z_2, z_3) \in \Omega = [-1, 1]^3$. Also we assume that $S(z_1, z_2, 0) = L_0$, $0 \leq z_1 \leq 1$, $0 \leq z_2 \leq 1$ and the solution of the Eikonal equation, which can be obtained in a similar way as in the two - dimensional case, will be

$$S(z_1, z_2, \sigma) = L_0 - \sigma, \quad 0 \leq z_1 \leq \sigma, \quad 0 \leq z_2 \leq \sigma.$$

In such a case for $A$ being now the area of the surface $\Gamma_s$ and $V_g$ the volume of the gypsum - void part of the cell, we have

$$A(y,\tau) \;=\; 6\left[4(L_0-\sigma(\tau))^2\right] = 6\left[4\left(L_0-\int_0^\tau W(y,\tau')d\tau'\right)^2\right],$$
$$V_g(y,\tau) \;=\; 8-8\left(L_0-\sigma(\tau)\right)^3 = 8-8\left[L_0-\int_0^\tau W(y,\tau')d\tau'\right]^3.$$

Then the field equation will have the following non-local form

$$\varepsilon W_\tau = W_{yy} + f_0 - \frac{1}{\gamma_m\phi_g}W\frac{3\left[L_0-\int_0^\tau W(y,\tau')d\tau'\right]^2}{\left[1-\left(L_0-\int_0^\tau W(y,\tau')d\tau'\right)^3\right]}, \quad (3.15a)$$

$$W(0,\tau)=\frac{1}{\phi(0,\tau)}, \qquad W_y(1,\tau)+\frac{\phi_y(1,\tau)}{\phi(1,\tau)}W(1,\tau)=0, \quad (3.15b)$$

$$W(y,\tau)=W_a(y), \quad (3.15c)$$

for $0<y<1$, $\tau\geq 0$.

*Spherical Segment.* In the case that the initial surface is that of a sphere of radius $R_0$ inside $\Omega$, we have that $\left(8-\frac{4}{3}\pi R_0^3\right)/8=\phi_c$, or $R_0=((1-\phi_c)(6/\pi))^{\frac{1}{3}}$. The solution for $S$ is $S(z_1,z_2,\sigma)=\left((R_0^2-\sigma)^2-z_1^2-z_2^2\right)^{\frac{1}{2}}$. More precisely we obtain

$$A(y,\tau) \;=\; 4\pi\left[(R_0-\sigma(\tau))^2\right] = 4\pi\left(R_0-\int_0^\tau W(y,\tau')d\tau'\right)^2,$$
$$V_g(y,\tau) \;=\; 8\left[R_0-\frac{4}{3}\pi\left(1-\sigma(\tau)\right)^3\right] = 8\left[R_0-\frac{4}{3}\pi\left(1-\int_0^\tau W(y,\tau')d\tau'\right)^3\right]$$

and the equation for $W$ takes the form

$$\varepsilon W_\tau = W_{yy} + f_0(y,\tau) - \frac{1}{\gamma_m\phi_g}W\frac{4\pi\left(R_0-\int_0^\tau W(y,\tau')d\tau'\right)^2}{8\left[1-\frac{4}{3}\pi\left(R_0-\int_0^\tau W(y,\tau')d\tau'\right)^3\right]}, \quad (3.16a)$$

$$W(0,\tau)=\frac{1}{\phi(0,\tau)}, \qquad W_y(1,\tau)+\frac{\phi_y(1,\tau)}{\phi(1,\tau)}W(1,\tau)=0, \quad (3.16b)$$

$$W(y,\tau)=W_a(y), \quad (3.16c)$$

for $0<y<1$, $\tau\geq 0$.

## 4. Numerical Solution

We deal with the Eikonal equation, (3.11) for the cases that we cannot have an analytical solution for it or if we have one but in an implicit form (e.g. see [15]), difficult to use in our case.

More specifically in order to treat numerically equation (3.11a) and (3.11b) we consider the grid $[0,1] \times [0,T_\sigma]$, where $T_\sigma$ is the final time of the simulation. We take $M_\sigma + 1$ points $z_{1j} = j\delta z_1$ for $\delta z_1$ being the spatial step for $j = 0, 1, 2, \ldots, M_\sigma$. In the interval $[0, T_\sigma]$, we take $N_\sigma$ time steps of size $\delta\sigma$ for $N_\sigma = [T_\sigma/\delta_\sigma]$ and with points of time discretization $\sigma_\ell = \ell\delta\sigma$, $\ell = 1, 2, \ldots, N_\sigma$.

We apply a standard upwind scheme (e.g. see [16], ch. 4) for the solution of the equation. By denoting with $S_j^\ell$ the approximation of $S(z_{1j}, \sigma_\ell)$ we have

$$S_j^{\ell+1} = S_j^\ell - \delta\sigma \left[1 + \left(\frac{S_j^\ell - S_{j-1}^\ell}{\delta z_1}\right)^2\right]^{\frac{1}{2}}, \quad j = 2, 3, \ldots, M_\sigma, \tag{4.1}$$

$$S_1^{\ell+1} = S_1^\ell - \delta\sigma, \quad \text{for} \quad j = 1,$$

and $\ell = 2, \ldots, N_\sigma$, while $S_j^1 = S_a(z_{1j})$. By getting the approximation of $S$, $S_\ell^j$ we are able to calculate the arclength of the curve $S$, i.e. $L = L(S^\ell) = L(\sigma_\ell)$, at each time step ($S^\ell = \left(S_1^\ell, S_2^\ell, \ldots, S_{M_\sigma}^\ell\right)$) by integration via e.g. the Simpson's rule. In addition the area occupied by cement, $A(S^\ell) = A(\sigma_\ell)$ is calculated in a similar way.

More specifically given the approximate solution of $S$ for each time step $\sigma_\ell$ we may calculate the approximations of $L$ and $A$. This is done by computing the integral $I_A(S^\ell) \simeq \int_0^1 S(z_1, \sigma_\ell) dz_1$. Also the arclength of $S^\ell$ can be calculated similarly by taking $I_L(S^\ell) \simeq \int_{S^\ell} S(z_1, \sigma_\ell) dz_1$.

The quantities $A(y_j, \tau_i) = A(\sigma_\ell)$ and $L(y_j, \tau_i) = L(\sigma_\ell)$ for some $\sigma_\ell$ are needed for evaluating the numerical solution of $W$ at each point $(y_j, \tau_i)$. To determine these quantities we proceed in the following way: At each point $(y_j, \tau_i)$ we calculate the quantity $I_{\tau_i}$ which is the approximation of the integral $\int_0^{\tau_i} W(y_j, \tau')d\tau'$. Then we have for some $\sigma$, $\sigma_\ell \simeq I_{\tau_i}$ and the proper index $\ell$ is taken to be the index of that $\sigma$ closest to $I_{\tau_i}$ i.e. that of one that minimizes the quantity $(\sigma_\ell - I_{\tau_i})$. In this way we evaluate $A(y_j, \tau_i) = I_L(\sigma_\ell)$ and for the same $\ell$, $L(y_j, \tau_i) = I_L(\sigma_\ell)$.

Having now the approximation for $S$ we may procced to the solution of the field equation. We apply a similar discetization as before in $[0, T] \times [0, 1]$, $0 \le \tau$, $0 \le y \le 1$ with $\tau_i = i\delta\tau$, $\delta\tau = [T/N]$ for $N$ the time steps and $y_j = j\delta y$, $j = 0, 1, \ldots, M$. Then we proceed with a finite element approach as in [9].

Let $\Phi_j$, $j = 0, \ldots, M$ denote the standard linear B - splines on the interval [0, 1], defined with respect to the partition considered.

$$\Phi_j = \begin{cases} \frac{y-y_{j-1}}{\delta y}, & y_{j-1} \leq y \leq y_j, \\ \frac{y_{j+1}-y}{\delta y}, & y_j \leq y \leq y_{j+1}, \\ 0, \quad \text{elsewhere in} \quad [0,\,1], \end{cases} \tag{4.2}$$

for $j = 0, 1, 2, \ldots, M$. We then set $W(y,\tau) = \sum_{j=0}^{M} a_{w_j}(\tau)\Phi_j(y)$, $\tau \geq 0$, $0 \leq y \leq 1$.

Substituting these expression for $W$ into equation (3.10a) with $f_0 = 0$ and applying the standard Galerkin method, i.e. multiplying with $\Phi_i$, for $i = 1, 2, \ldots, M$ and integrating over [0, 1], we obtain a system of equations for the $a_w$'s.

$$\begin{aligned} \varepsilon \sum_{j=0}^{M} \dot{a}_{w_j}(\tau) < \Phi_j(y)\,\Phi_i(y) > \quad &= -\sum_{j=0}^{M} a_{w_j}(\tau) < \Phi_j'(y)\,\Phi_i'(y) > \\ &+ \quad < F\left(\sum_{j=0}^{M} a_{R_j}(\tau)\Phi_j(y)\right)\Phi_i(y) >, \end{aligned} \tag{4.3}$$

where $< f, g >:= \int_0^1 f(y)g(y)dy$ and $i = 1, 2, \ldots, M$. Setting $a_w = [a_{w_1},\, a_{w_2}, \ldots, a_{w_M}]^T$ the system of equations for the $a_w$'s take the form

$$A\dot{a}_w(\tau) \;=\; -Ba_w(\tau) + b(\tau),$$

where, taking also into account the boundary conditions, (3.10b) and (3.10c), the matrices $A, B$ and $b$ have the form

$$A = \varepsilon\delta y \begin{bmatrix} \frac{2}{3} & \frac{1}{6} & 0 & \ldots & 0 \\ \frac{1}{6} & \frac{2}{3} & \frac{1}{6} & \ldots & 0 \\ 0 & 0 & \ddots & \ddots & 0 \\ 0 & 0 & \ldots & \frac{1}{6} & \frac{1}{3} \end{bmatrix}, \quad B = \frac{1}{\delta y} \begin{bmatrix} 2 & -1 & 0 & \ldots & 0 \\ -1 & 2 & -1 & \ldots & 0 \\ 0 & 0 & \ddots & \ddots & 0 \\ 0 & 0 & \ldots & -1 & \frac{\phi_y(1)}{\phi(1)} + 1 \end{bmatrix},$$

$$b(t) = \begin{bmatrix} \frac{1}{\phi(0)} + < F(R), \Phi_1 > \\ < F(R), \Phi_2 > \\ \vdots \\ < F(R), \Phi_M > \end{bmatrix}$$

We then apply a three time step approximation by taking $\dot{a}_w(\tau_n) \simeq \left(a_w^{n+1} - a_w^{n-1}\right)/(2\delta\tau)$. The corresponding equation then becomes

$$A\left(\frac{a_w^{n+1} - a_w^{n-1}}{2\delta\tau}\right) = -B\left(\frac{a_w^{n+1} + a_w^{n-1}}{2}\right) + b^n,$$

where $b^n = b(t_n)$.

After some manipulation we obtain the equations

$$a_w^{n+1} = (A + \delta\tau B)^{-1} \left[ (A - \delta\tau B) a_w^{n-1} + 2\delta\tau\, b^n \right]. \tag{4.4}$$

Note that for the second time step we have in place of equation (4.4) the following

$$a_w^2 = (A + \delta\tau B)^{-1} \left[ (A - \delta\tau B) a_w^1 + \delta\tau\, b^1 \right],$$

for $a_w^1$ being determined by the initial condition.

*Three - Dimensional Elements.* For the three - dimensional case we can easily modify the equation for $S = S(z_1, z_2, \sigma)$, with $z_3 = S(z_1, z_2, \sigma, )$, for $z = (z_1, z_2, z_3)$. More specifically we have

$$-\frac{\partial S}{\partial \sigma} = \sqrt{1 + \left(\frac{\partial S}{\partial z_1}\right)^2 + \left(\frac{\partial S}{\partial z_2}\right)^2}, \quad 0 < z_1, z_2 < 1, \quad \sigma \geq 0, \tag{4.6a}$$

$$\frac{\partial S}{\partial z_2}(z_1, 0, \sigma) = 0, \quad \frac{\partial S}{\partial z_1}(0, z_2, \sigma) = 0, \quad 0 < z_1, z_2 < 1, \quad \sigma \geq 0, \tag{4.6b}$$

$$S(z_1, z_2, 0) = S_a(z_1, z_2), \qquad 0 \leq z_1, z_2 \leq 1. \tag{4.6c}$$

We take $j_1, j_2 = 1, 2, \ldots, M_\sigma$, $z_{1j_1} = j_1 \delta z_1$, $z_{2j_2} = j_1 \delta z_2$, and $S^\ell_{j_1,j_2}$ being the approximation of $S(z_{1j_1}, z_{2j_2}, \sigma_\ell)$. The numerical scheme in this case will be

$$S^{\ell+1}_{j_1,j_2} = S^\ell_{j_1,j_2} - \delta\sigma \left[ 1 + \left( \frac{S^\ell_{j_1,j_2} - S^\ell_{j_1-1,j_2}}{\delta z_1} \right)^2 + \left( \frac{S^\ell_{j_1,j_2} - S^\ell_{j_1,j_2-1}}{\delta z_2} \right)^2 \right]^{\frac{1}{2}},$$

$$\text{for} \quad j_1, j_2 = 2, 3, \ldots, M_\sigma,$$

$$S^{\ell+1}_{1,j_2} = S^\ell_{1,j_2} - \delta\sigma \left[ 1 + \left( \frac{S^\ell_{1,j_2} - S^\ell_{J_1,j_2-1}}{\delta z_2} \right)^2 \right]^{\frac{1}{2}} \quad \text{for} \quad j_2 = 2, 3, \ldots, M_\sigma,$$

$$S^{\ell+1}_{j_1,j_2} = S^\ell_{j_1,1} - \delta\sigma \left[ 1 + \left( \frac{S^\ell_{j_1,1} - S^\ell_{j_1-1,j_2}}{\delta z_1} \right)^2 \right]^{\frac{1}{2}} \quad \text{for} \quad j_1 = 2, 3, \ldots, M_\sigma,$$

$$S^1_{j_1,j_2} = S_a(z_{j_1}, z_{j_2}).$$

## Numerical Simulations

In Figure 5, the system of equations (3.13) is solved numerically and the moving boundaries, $y_l(\tau)$ and $y_u(\tau)$, given by the conditions $\max\{\tau : A(y_l(\tau),\tau) = 4-(2L_0)^2\}$ and $\min\{\tau : A(y_u(\tau),\tau) = 4\}$ respectively, are plotted against time in (a). The same is done for the system of equations (3.14) in (b), for the moving boundaries given by the conditions $\max\{\tau : A(y_l(\tau),\tau) = 4-\pi R_0^2\}$ and $\min\{\tau : A(y_u(\tau),\tau) = 4\}$. Finally problem (3.10) is solved for the case that the initial boundary of the calcite segment has the form of a Lamé curve as in Figure 3(c). More specifically we used the curve $x^n/c_1^n + y^n/c_2^n = 1$ for $n = 6$ and $c_1 = 1$ and $c_2$ such that $4 - A(y,0)/4 = \phi_c$ for $\sigma = 0$. In all of these simulations we assume that $f_0 = 0$ and that $\mathrm{SO}_4^{2-}$ diffuses inside the pores while its concentration at the boundary $y = 0$ remains constant.

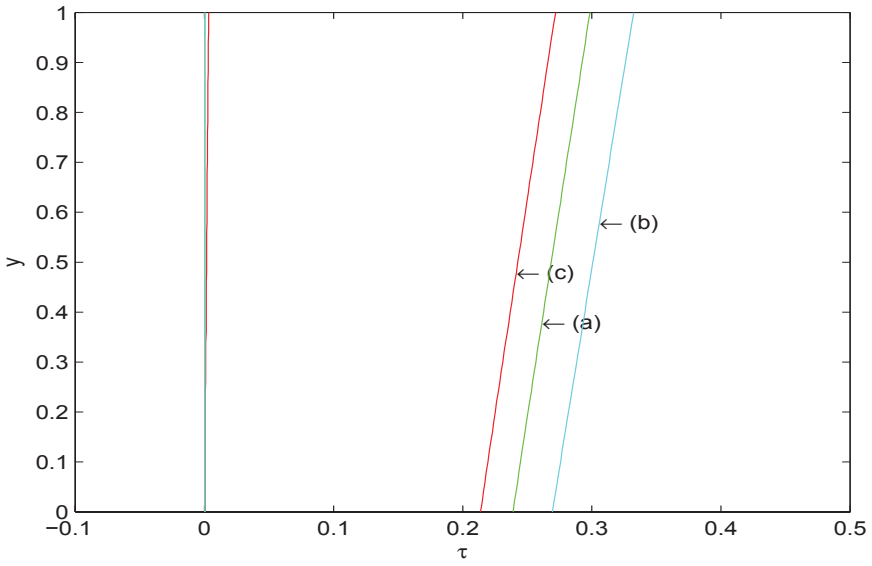


*Figure 5. Moving boundaries, indicating when the corrosion is complete in the cases of having an initial calcite element in the form of (a) a square, (b) a cycle and (c) a Lamé curve.*

In Figure 5 we see plots of the macroscopic moving boundaries $y_u$ and $y_l$. The $y$ axis corresponds to the macroscopic length of the material. The area between $y_l$ and $y_u$ indicates the mushy region. The boundary $y_l$ describes, e.g. thinking of the sewer pipe corrosion situation, the motion of point C in Figure 1, while, in the same context, $y_u$ describes the motion of point B.

As we can see in Figure 5 the numerical results indicate that, for a smooth surface the curvature of the initial curve may be a factor that slows down the process since we notice that the material with cyclical calcite segments is corroded at a later time compared with the others. Note also that in similar experiments, where an initial Lamé curve of the form $z_1^n/c_1^n + z_2^n/c_2^n = 1$ is taken, we notice that the corrosion becomes faster if we increase the exponent $n$. In the case of the non smooth square initial curve, and perhaps due to the corner singularities, we notice a different behaviour of the corrosion speed, placing the corresponding boundary (a) before that of the circle (b) and after the one of the Lamé curve (c).

Also we notice that corrosion starts almost instantly for every $y$ in $[0, 1]$, i.e. in every cell of the material, since for every $y$ the boundary $y_l$ remains very close to the $y$-axis. There is a small deviation, visible in case (c), of $y_l$ as we approach $y = 1$ meaning that for some small time the cells corresponding to $y$ close to one remain uncorroded, as in Figure 2a. Due to diffusion of $SO_4^{2-}$, from $y = 0$ where its concentration is constant, the amount of $SO_4^{2-}$ is larger near this point compared with the points away from it, therefore the rate of the reaction is faster there and consequently the cells near this point are also being corroded faster. Near the point $y = 1$ and since initially we have $W = 0$ and no source term, it needs some time for the sulphate to become non-zero and to initiate the reaction. For the times that we are right of $y_l$ the cells corresponding to each $y$ are partly corroded and correspond to the form of Figure 2b.

To see a more visible variation in $y_l's$ we need a larger $\varepsilon$ to slow down the diffusion process.

Then at later times, for example in (c) case, at about 0.21 time units and for $y = 0$ the moving boundary $y_u$ initiates, indicating that all the cells corresponding at the point $y = 0$ have been fully corroded and that its calcite have been transformed fully into gypsum. At about 0.25 time units the moving boundary $y_u$ reaches the point $y = 1$. This means that now the whole of the material and even the cells corresponding to this point, have been fully corroded and that the calcite contained in the cells has been fully transformed to gypsum while these obtain the form of Figure 2c .

The values of the parameters used in these simulations are for $M = 51$, $T = .5$, $\epsilon = 1$, $\gamma_m = 1$, $\phi_c = 0.3$, $\phi_g = 0.4$, $\delta\tau = .8 \cdot \delta y^2$, $M_\sigma = 41$, $\delta\sigma = .1 \cdot \delta z_1$, $T_\sigma = 1$.

Furthermore problem (3.10) is solved numerically again but now for the inverse case that we have a cyclical pore centred inside a square cell. The radius of the pore should be such that $\pi R_0^2/4 = \phi_c$. Then as the process evolves the boundary of the calcite $\Gamma_c$ is approaching the

boundary of the square element $\Gamma_e$. To address this behaviour we take the opposite sign in equation (3.10d). For $S$ increasing we have

$$\frac{\partial S}{\partial \tau}\frac{1}{\sqrt{1+\left(\frac{\partial S}{\partial z_1}\right)^2}} = W(y,\tau), \quad 0 < y,\, z_1 < 1, \quad \tau \geq 0. \tag{4.7}$$

The solution is demonstrated in Figure 6. In Figure 6(a) $W(y,\tau)$ and in 6(b) $A(y,\tau)$ are plotted against space and time. The values of the parameters used are the same as those for Figure 5. We notice that

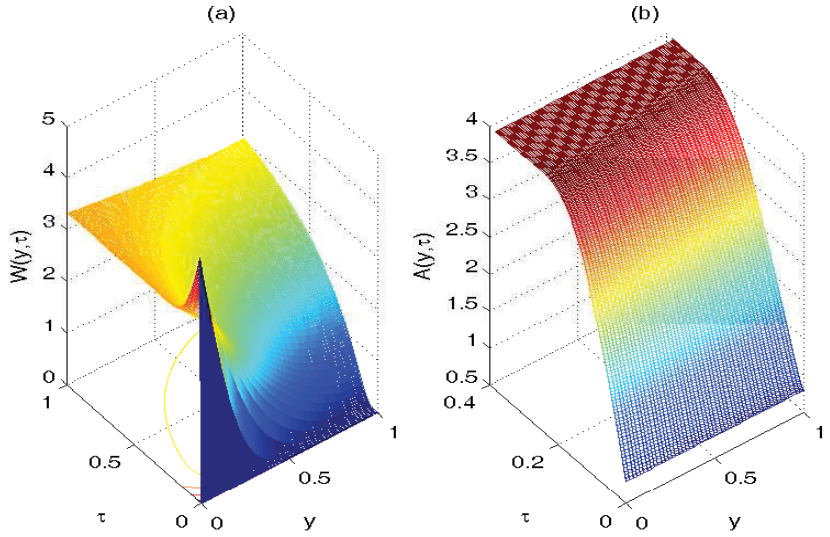


*Figure 6. Numerical solution of problem (3.10) but with an increasing $S$ given by equation (4.7). In (a) $W(y,\tau)$ and in (b) $A(y,\tau)$, are plotted against space and time.*

the area of the gypsum- void system is increasing until it occupies the whole square element, i.e. $A(y,\tau) = 4$.

Similar simulations can be done for the three-dimensional case, as for instance in Figure 7. The system of equations (3.15) is solved numerically and the moving boundaries given by the conditions $\max\{\tau : V_g(y_l(\tau),\tau) = 8 - (2L_0)^3\}$ and $\min\{\tau : V_g(y_u(\tau),\tau) = 8\}$ are plotted against time in (a). In (b) for the case that we consider initially spherical elements of calcite we solve numerically problem (3.16). Finally in (c) problem (3.10), but with equations (4.6) in the place of equations (3.10d), (3.10e) and with the equations (3.10f), (3.10g) modified appropriately, is solved for the case that the initial boundary of the calcite segment is surrounded by the surface $z_1^n/c_1^n + z_1^n/c_2^n + z_1^n/c_3^n = 1$. The parameters used are $n = 6$, $c_1, = c_2 = 1$ and $c_3$ chosen so that

$8 - V_g(y,0)/8 = \phi_c$. Also in equation (3.10a) we consider the volume $V_g$ and area $A$ of the corresponding three dimensional surface in place of $A$ and $L$ respectively. The values of the parameters used are the same as for Figure 5.

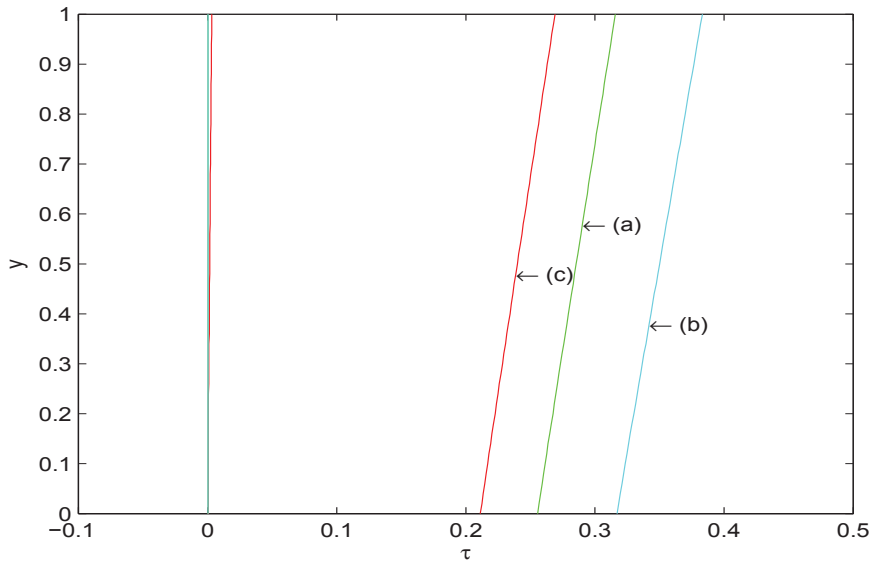


*Figure 7. Moving boundaries, indicating when the corrosion is complete in the cases of having an initial calcite element in the form of : (a) a cube, (b) a sphere and (c) a Lamé surface.*

The results are similar as in the two-dimensional case. Spherical calcite segments take more time to be corroded and in all of the cases the corrosion process starts instantly in the whole of the domain.

Finally in Figure 8 the shrinking of a sphere is presented as being a solution of equations (4.6). The parameters used here are $M_\sigma = 41$, $\delta\sigma = 0.1\,\delta z_1$, $\delta z_1 = \delta z_2$, $T_\sigma = 1$.

*Application for the case of sewer pipes corrosion.* We use this modelling approach to simulate the sewer pipes corrosion example presented in the introduction. In such a case the system to be solved is given by the equations (2.4a) and (2.4b) together with the modified version of (2.4c) in which now the source term representing the reaction, derived by the averaging procedure, has to be added. Thus we obtain

$$\epsilon_3 \frac{\partial W}{\partial \tau} = \frac{\partial^2 W}{\partial y^2} + \beta_3 V + F(W), \tag{4.8}$$

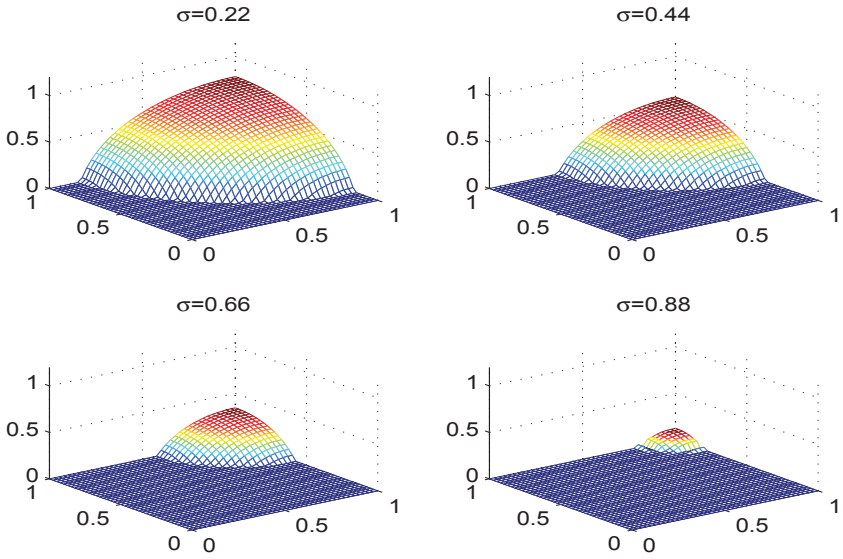


*Figure 8. A shrinking spherical calcite element presented for various values of time $\sigma$.*

with $F(W)$ given by

$$F(W) = -\frac{1}{\gamma_m \phi_g} W \frac{L(y,\tau)}{A(y,\tau)},$$

together with (3.10b) to (3.10g). Also the boundary and initial conditions for $U$ and $V$ need to be given in a similar way as for $W$ i.e. by (3.10b) and (3.10c) with $U$ or $V$ instead of $W$. The system can be solved numerically by applying the methodology presented in the beginning of this section and basically given by equation (4.3) and for the cases that we don't have an analytical solution for the Eikonal equation, also by (4.1).

More interesting is the case where we use specific values of the parameters (cf. [1, 9]) leading to small values for $\epsilon$ and large values for $\mu$. More specifically, we have $\epsilon_1$, $\epsilon_2$, $\epsilon_3 \ll 1$ and $\mu_1$, $\mu_2 \gg 1$, $\beta_1 = 1$, giving $U \sim V$ and allowing us to apply the *quasi steady approximation*. In such a case the model equations to be solved become

$$\frac{\partial^2 V}{\partial y^2} - \beta_2 V = 0, \tag{4.9a}$$

$$\frac{\partial^2 W}{\partial y^2} + \beta_3 V + F(W) = 0, \tag{4.9b}$$

together with the boundary conditions for $V$ and $W$ and the equations for the $S$-problem as already specified. The finite element method can be easily applied to this case, as in [9] and the results for the various microscale geometries is presented in Figure 9. As we can see in these simulations corrosion is faster in the two dimensional geometries and more specifically in the case of the boundary being a Lamé curve, next being a square, then being a cycle, but with the exterior being the calcite, and finally being a cycle. The same ordering is followed in the three dimensional case with the case of the sphere needing the larger time for the material to be corroded. The latter case seems to be more realistic if we take into account the simulations done in [1] and [9].

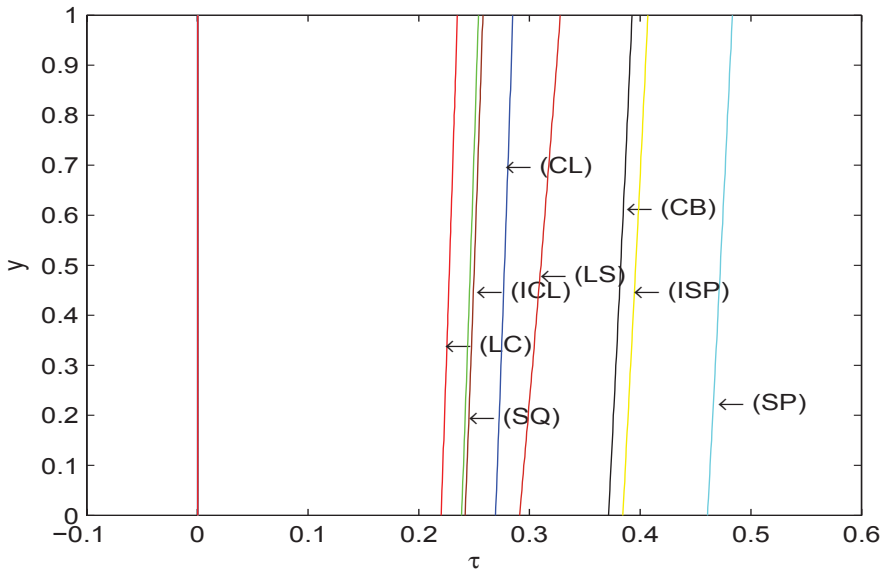


*Figure 9. Form of the moving boundaries indicating the completion of corrosion for various geometrical considerations. More specifically for the cases that the calcite boundary is a) Lamé curve (LC), b) square (SQ), c) cycle (CL), (d) cycle but with the exterior being the calsite (ICL), e) Lamé surface (LS) f) cube (CB) g) sphere (SP) and h) surface of a sphere but with the exterior being the calsite (ISP)*
*The values of the parameters that were used were* $\beta_2 = 2.3275, \beta_3 = 2.3741\,10^{-5}$, $\gamma_m = 6.78$, $\gamma = 67.8$, $\phi_c = 0.2$, $\phi_g = 0.3$, $M = 61$, $\delta\tau = 0.8 \cdot \delta y^2$, $M_\sigma = 101$, $\delta\sigma = 0.1 \cdot \delta {z_1}^2$.

## 5. Conclusions

In this paper a mathematical model for the formation of a mushy region in concrete during corrosion by $H_2SO_4$ is further studied and improved.

The same basic model presented in [9] is significantly improved by including the Eikonal equation describing the evolution of the moving boundary at each time. In the cases we have analytical solutions of the Eikonal equation, we may proceed further and obtain a simplified version of the model in the form of a non-local reaction diffusion equation.

In addition the problem is solved numerically, for various microgeometries, with the use of a finite element method. The results by these simulations are presented and predict corrosion within a reasonable range.

This work can be further extended by relaxing some of the assumptions used here. For instance one possible extension can arise by considering that the microstructure elements, the cells, are not all of them of the same form and not having the same initial calcite shape (e.g. local periodicity of cells replacing the usual uniform periodicity like in [5]). A distribution of these formations might be adapted in the model, giving more realistic results. In general, as also it is stated in [9], more complicated considerations for the geometry of cracks, as in [12] where the melting of an alloy is studied, together with the development of its fractal structure ([17], [18]) can extend further this work.

The inclusion of the volume expansion of the material due to the transformation of the calcite to gypsum which has lower density, is an important aspect that should be studied in the present context of the two scale approach, as first step before studying the corresponding mechanical deformation.

It would be also of interest to proceed with a more rigorous setting for the formal asymptotics presented here as it is done in [5]-[8] but for a system of reaction diffusion equations with fixed boundaries.

Finally more accurate evaluation of the parameters can give better results and possible lead to further variations for the models (e.g. as the case of having $\epsilon$ of $O(\delta)$ or smaller etc.).

## Acknowledgements

The author wants to thank Professor A. A. Lacey for having a very useful discussion regarding this work.

## References

1. M. Böhm, J. Devinny, F. Jahani, G. Rosen, (1998), *On a moving-boundary system modelling corrosion in sewer pipes*, Applied Mathematics and Computation, 92: 247–269.

2. A. Fasano, R. Natalini (2006) *Lost Beauties of the Acropolis : What Mathematics Can Say*, SIAM News, 39, July/August 2006.
3. M. Bohm, J. S. Devinny, F. Jahani, F. B. Mansfeld, I. G. Rosen, C.Wang, (1999), *A Moving Boundary Diffusion Model for the Corrosion of Concrete Wastewater Systems: Simulation and Experimental Validation*, Proceedings of the American Control Conference San Diego, California, June 1999: 1739–1743.
4. M. Böhm, and I. G Rosen, . (1997) *Global weak solutions and uniqueness for a moving boundary problem for a coupled system of quasilinear diffusion-reaction equations arising as a model of chemical corrosion of concrete surfaces*, Institut fur Mathematik, Humboldt-Universitat, Berlin.
5. T. Fatima, N. Arab, E. P. Zemskov, A. Muntean, (2011) *Homogenization of a reaction - diffusion system modeling sulfate corrosion of concrete in locally periodic perforated domains*, Journal of Engineering Mathematics, 39(2-3): pp 261–276.
6. T. Fatima, A. Muntean, (2013) *Sulfate attack in sewer pipes: Derivation of a concrete corrosion model via two-scale convergence* Nonlinear Analysis: Real World Applications, DOI:10.1016/j.nonrwa.2012.01.019,2013.
7. T. Fatima, A. Muntean, T. Aiki, (2012), *Distributed space scales in a semilinear reaction-diffusion system including a parabolic variational inequality: A well-posedness study*, Adv. Math. Sci. Appl., 22(1): 295–318.
8. T. Fatima, A. Muntean, M. Ptashnyk, (2012), *Unfolding-based corrector estimates for a reaction - diffusion system predicting concrete corrosion*, Applicable Analysis, 91(6): 1129–1154.
9. C. V. Nikolopoulos, (2010) *A Mushy Region in Concrete Corrosion*, Applied Mathematical Modelling, 34: 4012–4030.
10. A.A Lacey, L.A. Herraiz, (2002), *Macroscopic models for melting derived from averaging microscopic Stefan problems I: Simple geometries with kinetic undercooling or surface tension* . Euro. Jnl. of Applied Mathematics, 11: 153–169.
11. A. Jaklic, A. Leonardis and F. Solina, (2000) *Segmentation and Recovery of Superquadrics*, Computational imaging and vision, Vol. 20, Kluwer, Dordrecth.
12. A.A Lacey, L.A. Herraiz, (2002), *Macroscopic models for melting derived from averaging microscopic Stefan problems II: Effect of varying geometry and composition*. Euro. Jnl. of Applied Mathematics, 13: 261–282.
13. E. J. Hinch, (1991) *Perturbation Methods*, Cambridge University Press.
14. S. Howison, A.A. Lacey, Movack, J. Ockendon, (2003) *Applied Partial Differential Equations*, Oxford University Press.
15. E. D. Moskalensky, (2009), *Finding Exact Solutions to the Two-Dimensional Eikonal Equation* Numerical Analysis and Applications, 2: 165–172.
16. R. J. Leveque,(2002),*Finite Volume Methods for Hyperbolic Problems*, Caimbridge University Press.
17. B Chiaia, J. G. M. van Mier, A. Vervuurt,(1998), *On the fractal dimension of fracture surfaces of concrete elements*, Cement and Concrete Research, 28(1): 103–114.
18. G. M. Idorn, (2005), *Innovation in concrete research review and perspective*, Cement and Concrete Research, 35: 3–10.